Inertial electrostatic confinement and DD fusion at interelectrode media of nanosecond vacuum discharge. PIC simulations and experiment

2009 J. Phys. A: Math. Theor. 42 214041

(http://iopscience.iop.org/1751-8121/42/21/214041)

IOP PUBLISHING JOURNAL OF PHYSICS A: MATHEMATICAL AND THEORETICAL

J. Phys. A: Math. Theor. **42** (2009) 214041 (9pp) doi:10.1088/1751-8113/42/21/214041

Inertial electrostatic confinement and DD fusion at interelectrode media of nanosecond vacuum discharge. PIC simulations and experiment

Yu K Kurilenkov[1], V P Tarakanov[1], M Skowronek[2], S Yu Guskov[3] and J Dufty[4]

[1] Joint Institute for High Temperatures of Russian Academy of Sciences, 13/19 Izhorskaya Str, 125412 Moscow, Russia
[2] Laboratoire des Plasmas Denses, Université Pierre et Marie Curie, F-75252 Paris, Cedex 05, France
[3] Lebedev Physics Institute, 119991 Moscow, Russia
[4] Department of Physics, University of Florida, Gainesville, FL 32611, USA

E-mail: yukurilenkov@rambler.ru, maurice.skowronek@noos.fr, guskov@fci.lebedev.ru and dufty@phys.ufl.edu

Received 17 October 2008, in final form 24 October 2008
Published 8 May 2009
Online at stacks.iop.org/JPhysA/42/214041

Abstract

The generation of energetic ions and DD neutrons from microfusion at the interelectrode space of a low-energy nanosecond vacuum discharge has been demonstrated recently [1, 2]. However, the physics of fusion processes and some results regarding the neutron yield from the database accumulated were poorly understood. The present work presents a detailed particle-in-cell (PIC) simulation of the discharge experimental conditions using a fully electrodynamic code. The dynamics of all charge particles was reconstructed in time and anode–cathode (AC) space. The principal role of a *virtual cathode* (VC) and the corresponding single and double potential wells formed in the interelectrode space are recognized. The calculated depth of the *quasistationary potential well* (PW) of the VC is about 50–60 keV, and the D^+ ions being trapped by this well accelerate up to energy values needed to provide collisional DD nuclear synthesis. The correlation between the calculated potential well structures (and dynamics) and the neutron yield observed is discussed. In particular, ions in the potential well undergo high-frequency (∼80 MHz) harmonic oscillations accompanied by a corresponding regime of oscillatory neutron yield. Both experiment and PIC simulations illustrate favorable *scaling of the fusion power density* for the chosen IECF scheme based on nanosecond vacuum discharge.

PACS numbers: 52.80.Vp, 52.58.Qv, 52.65.Rr, 52.40.Mj, 52.27.Lw

(Some figures in this article are in colour only in the electronic version)

1. Introduction

Generally, the efficiency of hard x-rays and fast ions generation by nanosecond vacuum discharge, as well as the neutron generation, is at least two orders of magnitude higher [1, 2] than for experiments on DD fusion driven by the Coulomb explosion of laser-irradiated deuterium clusters [3]. However, the complex physics of nanosecond discharge processes and the mechanisms of microfusion are poorly understood, and motivated the interest in complementary particle-in-cell (PIC) simulations [4]. In addition to representing the key points of the general physical picture, computer modeling allows clarification of the details of the experimental data, such as the appearance of double neutron peaks or pulsating neutron yield.

The model of collective ion acceleration [5] at a vacuum discharge, based on the concept of *nonstationary* potential wells (PW) before the front of the cathode flare in the regimes of non-stable current carrying, was developed rather recently [6]. On the basis of this model, explanations were provided for the early experimental data of A A Plyutto and coauthors [7] on occasional anomalous ions acceleration. Our results of PIC simulations of the experimental setup [2] using the axisymmetrical version of the electrodynamic code KARAT [4] have recognized that the concept of PW is more universal; namely, a *quasistationary* PW at interelectrode space with a depth up to ∼80% of the applied voltage (70 kv) provides electrostatic acceleration of ions up to the same energies. Correspondingly, head-on collisions of ions with energies of a few tens of keV is followed by DD nuclear synthesis, transforming the interelectrode space into something like a reactor chamber.

In fact, PIC modeling allows the identification of the experiment [1, 2] with a rather old branch of plasma physics, as inertial electrostatic confinement fusion (IECF) (see [8–12] and references therein). Pioneers of IECF were O Lavrent'ev in the USSR and F Farnsworth in the US, but due to different reasons, including a rather low value for $Q = E_{\text{fusion}}/E_{\text{input}} \sim 10^{-6}$–$10^{-5}$, this concept for fusion was almost forgotten. Just during the last decade, interest in IECF was renewed at US and Japan mainly as a simple source of neutrons [10–12]. Furthermore, some modern experimental set-ups under the study and construction at LANL provide new expectations to get $Q > 1$ [12] (as a minimum in theory).

2. Virtual cathode and potential wells

To explain the nature of fusion in experiments with nanosecond vacuum discharge [1, 2], just a limited number of PIC 2D calculation results are discussed below. In particular, figure 1 represents an example of calculations of the particle dynamics for a cylindrical geometry, and demonstrates the appearance of the VC. Related to the VC, examples of PWs are shown in figures 2 and 3 for different times of the discharge pulse (the A–C configuration follows easily from these figures). Note that for the experimental conditions [2], the cylindrical Cu anode ($\varnothing = 0.6$ cm) has a set of thin hollow Pd deuterated tubes ($\varnothing = 0.1$ cm) attached to anode end-on, and the hollow cathode was constructed from Al [13]. The simulation region contains on the left side the coaxial waveguide with the central anode ended by semitransparent 'foil' corresponding to Pd tubes. The outer cathode of the coax has the region emitting electrons in the direction of axes through the foil. Initially the plasma corresponding to eroded tube material is loaded in place of foil. The remains of anode 'erosion plasmas' there are as the small green sphere at the center of the 'void' in figure 1, where $V_r/c \approx 0$ and $r \approx 0.3$ cm. When voltage to the coax is applied, electrons are extracted from the internal surface of the cathode ($r \approx 0.4$–0.6 cm) and accelerated up to $v_{\text{e-max}} \approx 0.3c$–$0.4c$ near Pd tubes ($r = 0.3$ cm). The interaction of electron beams with tubes provides erosion of the system (Pd + D_2)

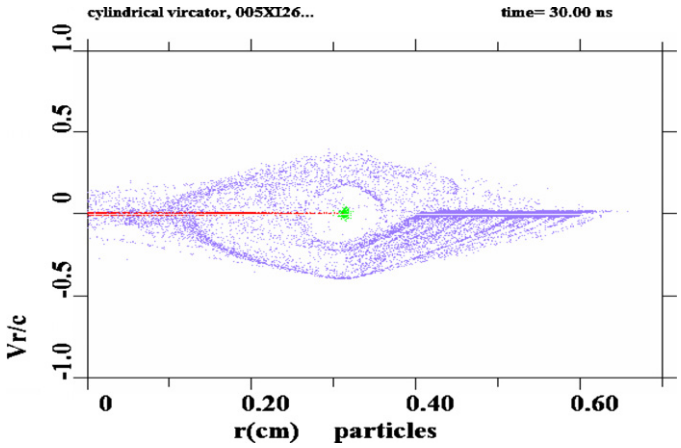

Figure 1. Particle dynamics and virtual cathode formation by PIC modeling (radial velocities of particles as function of radius value: blue—electrons, red— deuterium ions, green area—anode erosion plasma with deuterium; c is the velocity of light).

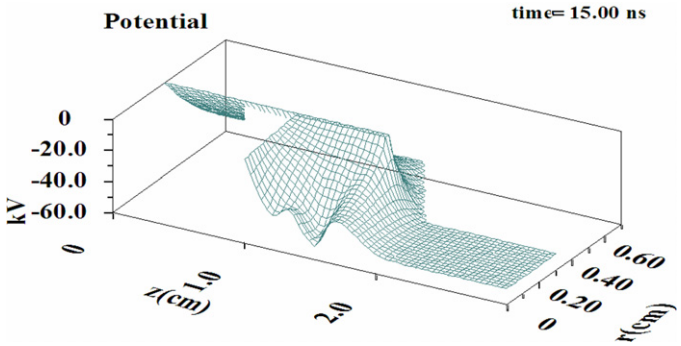

Figure 2. Double potential well (PW), appearing at the first part of voltage pulse applied.

and ejection (implosion) of deuterium and palladium vapors into the near anode axis area (accompanied by their partial nucleation in a real experiment). Further, since the electron current I_A exceeds the limiting Childe–Langmuir–Boguslavski value, $I_A > I_L$ [14], cumulative convergence of head-on e-beams at the axis (inside the space restricted by Pd tubes) provides total deceleration of electrons (as well as partial reflection of electrons outside, $V_r/c > 0$), and the VC appears (at $r \approx 0.1$ cm).

A negative potential of about a few tens of keV corresponding to VC will appear at the axis (at $Z \approx 1.2$–1.8 cm), and the internal near-axis part will attract ions from anode area. The VC area will be filled by accelerated ions (figure 1, the red horizontal line $V_r/c \approx 0$ at $r = 0$–0.3 cm interval; this line will be split, in the ion scale of velocities, at $r = 0$ (on the Z-axis) into two head-on converged branches of ions with velocities $V_r^i/c = \pm 0.5 \times 10^{-2}$). The PW is evolving in time and can transform from a double well (figure 2) into broad single well (figure 3). The well depth is up to 80% of the applied voltage. It is interesting that ions being strongly coupled near PW edges ($\Gamma \gg 1$) are accelerating from different edges to the Z-axis, and represent there the ideal ions head-on fluxes ($\Gamma \approx 0$) at $r \to 0$ with ion energies of 20–50 keV. Evidently, this explains the collisional DD fusion observed in the real experiments (in that case, we also have

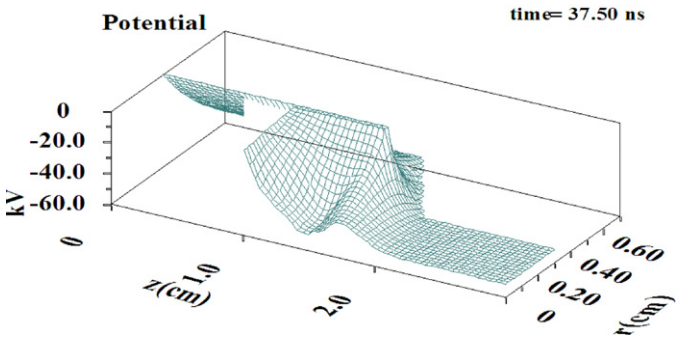

Figure 3. Typical deep single potential well along the *Z*-axis, at 37.5 ns (PW minimum corresponds to $Z \approx 1.5$ cm).

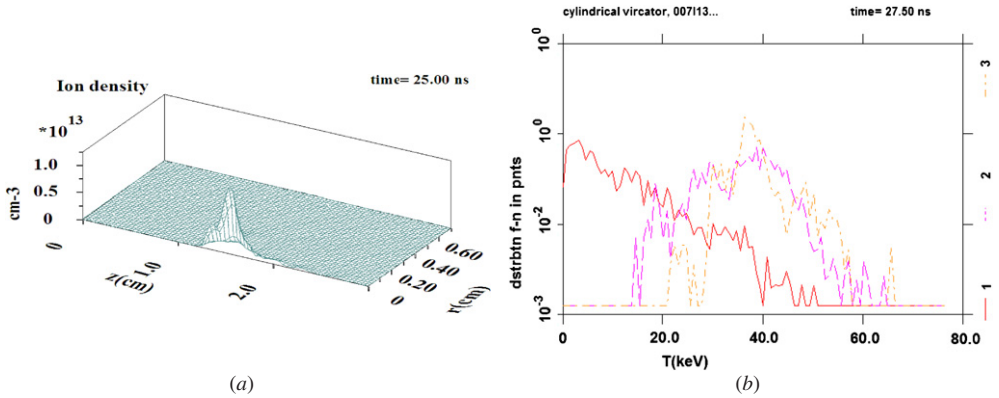

(*a*) (*b*)

Figure 4. (*a*) Example of average density of fast ions in potential well (along the discharge axis *Z*; $Z = 1$ is the edge of the Cu anode). (*b*) Distribution function for accelerated ions at different areas along the radius ($1 - r = 0.3$ cm, $2 - r = 0.2$ cm, $3 - r = 0.0$ cm; in the plane of PW minimum, $Z \approx 1.5$ cm).

to take into account collisions with neutrals, deuterium clusters and the deuterated anode itself) [2]. The area of *Z* and *r* at the half-width of the PW contains an almost isotropic distribution of fast ions (volume of the 'reactor'). The ion density has a maximum at the bottom of the PW ($Z \approx 1.5$ cm) and a particular Gaussian-like shape is shown in figure 4 (absolute values of $n_{i\,\max}$ for the modeling will depend on the parameters of 'anode plasma' variation and especially of radial ion plasma compression ratio $\theta(t) = r_{\max}/r_{\min}$ changing in time).

3. Specifics and regimes of neutron yield

PIC simulations have assisted in understanding some effects observed in the earlier experiments [2]. For example, the shapes of some PIC non-Maxwellian distribution functions (figure 4(*b*)) are in correlation with a 'plateau' in histograms for fast ion tracks observed in the experiments (see figure 8 of [2]). Another example, well reproducing experiments by simulations, is the double potential wells in the first stage of discharge (as in figure 2; remark, double PW by the *Z*-axis, and weakly double by *r*, last one takes place and for single PW by *Z*). It looks very probable that the appearance of double wells might explain the double neutron

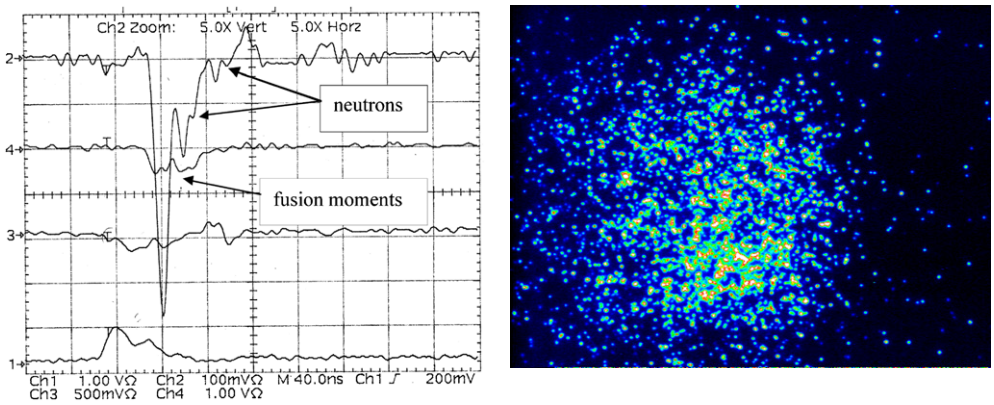

(*a*) (*b*)

Figure 5. (*a*) Oscillograms of hard x-ray yield (channels 1, 3 and 4) and neutron yield (double peaks, channel 2) (see the text and experiment [2]). (*b*) Hard x-ray CCD image of corresponding interelectrode ensemble.

peak observed sometimes in the experiment (as in figure 5, channel 2). We can see that the PW lifetime in the experiment is about $T_{\mathrm{PW}} \approx 20$–$25$ ns, and after that the VC has to be neutralized $\left(T_{\mathrm{PW}} \gg \omega^{-1}{}_{\pi}\right)$ by the flux of ions. Since the total pulse T_{pulse} of voltage is about 50 ns, there are sufficient conditions for the VC appearing in the experiments again ($I_A > I_L$), and a new double PW will appear. Ion collisions at this PW will be manifested by a second double neutron peak as shown in figure 5. Note that the appearance of single, double and multiple PWs, and non-Maxwellian distributions of ions are typical features of systems with IECF. Earlier, the study of correlations between PW structures and neutron yields has recognized that not only well depth, but namely potential instability in time defines the neutron yield in ion beam interactions [10].

In our experiments also, not only the PW structure but also the dynamics of potential will define the character of the neutron yield. As a result, three types of observed neutron yield could be recognized in the experiments [2]:

(1) single peaks (as in figures 2 and 5 of [2]), (2) multiple intermittent neutron yield (two and more neutron peaks, figure 5 above, and figures 3 and 7 of [2]), (3) oscillatory or pulsating neutron yield (as in figures 4 and 6 of [2], as well as in figures 6 and 7 below).

Let us consider the first two types of neutron yields. As shown in [6], the time taken to form the VC (or the decay time of potential) is about $T_v \approx C_d\, U/I_{L,}$ where C_d is the diode gap capacitance and U is the potential. Since $I_L \sim U^{3/2}/d^2{}_{\mathrm{eff},}$ then variation of d_{eff} in our experiment [2] changes I_L and, correspondingly, the value T_v (d_{eff} is the effective interelectrode distance for non-planar electrodes) [13]. Thus, at rather large d_{eff} we have $T_v \approx T_{\mathrm{pulse}}$, and just a single peak will be observed in experiments (first type). Decreasing d_{eff} increases I_L and lowers T_v, and step by step at decreasing of $T_v < T_{\mathrm{pulse}}$ we get double, and multiple neutron yields (second type). At $U = 50$ kV, $I_A/I_L \approx 1.5$, $C_d \approx 300$ pF [2] giving $T_v \approx 28$ ns. This is not far from the time taken to form the VC for the experimental case presented in figure 5.

The third type of neutron yield is of special interest. At $I_L \to I_A$, if the electron distribution in the VC would be close to uniform and the PW would still be present, then ion oscillations at the PW will be approximately harmonic. At the moments of maximum periodic compression of the ionic subsystem, the DD reaction will take place and the neutron yield will be a pulsating one (a typical example is shown in figure 6, channel 2 below and figures 4 and 6 of [2]). The period of oscillations of the neutron yield is about 12–13 ns in the experiments [2] ($T_v \ll T_{\mathrm{pulse}}$),

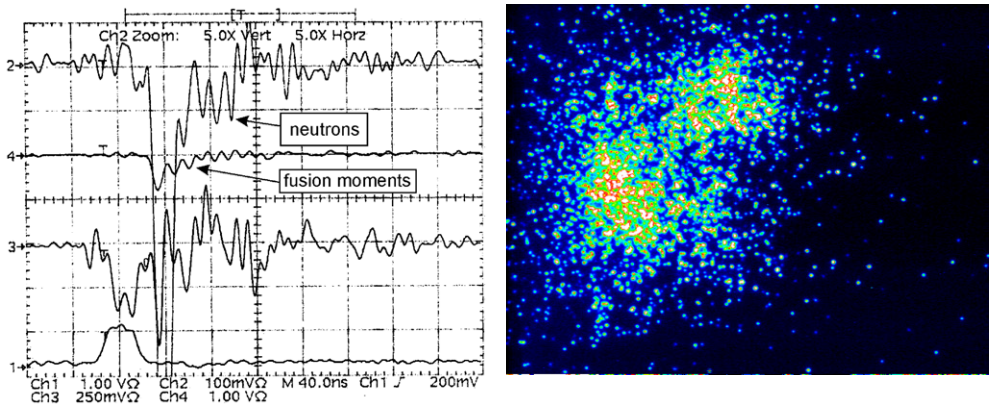

(*a*) (*b*)

Figure 6. (*a*) Oscillograms of hard x-rays intensities (channels 1, 3 and 4) and pulsating (oscillatory) regime of neutron yield (channel 2, see the text). Intensity of x-rays at channel 4 is modulated by the moments of DD fusion. (*b*) Hard x-ray CCD image of dilute interelectrode ensemble.

and it represents now mainly the frequency of harmonic oscillations D^+ in the PW (figure 3) instead of T_v (as for the first type of neutron yield). In fact, the pulsating neutron yield is appearing in the experiment just as d_{eff} is decreasing. Note that ion trajectories and energies obtained from PIC simulations for this particular experimental regime, figure 6, correspond namely to their periodic oscillations (ions acceleration–deceleration) at PW accompanied by periodic self-compression of the ionic subsystem at the axis of discharge. In summary, neutron yield as a single peak is the result of a single collapse of ions at the well bottom at neutralization of VC in the regime $T_v \approx T_{\text{pulse}}$, and the second type of yield is an intermediate one between single and multiple (oscillatory) yields at $I_L \to I_A$ (figure 6).

4. Comparisons and concluding remarks

The pulsating neutron yield regime (figure 6) is suggestive of the interesting and stimulating conception of periodically oscillating plasma spheres (POPS), developed successfully during the last decade in theory and in the experiment [11, 12]. There, it was suggested to abandon the standard scheme of IECF, where particular ion beams interact with each other, and use in addition the injection of electrons into grids (in order to get a uniform electron background inside the cathode grids). Ions then will undergo radial harmonic oscillations with any amplitude at the potential well formed, and at the moments of maximal compression high fusion power will be provided $P_{\text{fusion}} \approx 3\varphi^2\theta^2 f^2\langle\sigma\upsilon\rangle/2\pi e^2 r_{\text{VC}}$, where φ is the well depth, θ is the level of compression, $f = n_i/n_{\text{e}}$, r_{VC} is the radius of VC, and $\langle\sigma\upsilon\rangle$ is the averaged cross section (here P_{fusion} is the total power integrated over a single period [11]). A typical POPS frequency is $\nu_{\text{POPS}} \sim (2\varphi/m_i)^{1/2}/r_{\text{VC}}$ (m_i is the ion mass). Analysis of POPS physics has shown that a potential well depth of about 60% of the applied voltage and $\nu_{\text{POPS}} \sim 10$–$30$ MHz (DD) are enough for realization of the concept of a reactor in oscillating systems. However, at the present moment in spite of POPS attractiveness and demonstration ones, in principle, the PW depth reported is still $\leqslant 1$ keV, and POPS frequency $\nu_{\text{POPS}} \leqslant 1$ MHz (applications, economy, limitations are discussed in detail in [12]).

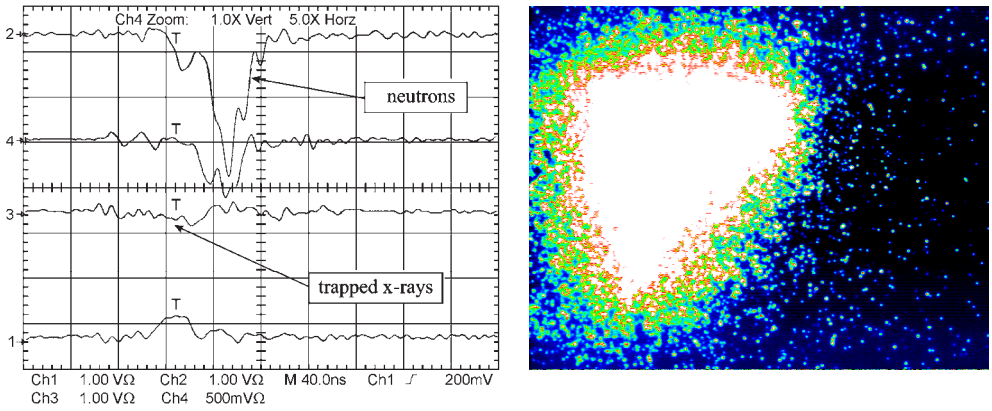

Figure 7. (*a*) Oscillograms of x-rays yield (channels 1 and 3) and neutron yields (channel 2) for specific interelectrode ensemble with trapped fast ions and x-rays (see text and [2] for details of experiment). (*b*) CCD image of corresponding self-organized cluster ensemble (complex plasma microreactor).

Generally speaking, POPS are particular and well-defined cases or analog of the *multiple fusion events* (MFI) [2] at vacuum discharge in the regime $T_v \ll T_{\text{pulse}}$ discussed above. In fact, instead of special injections of electrons into a spherical device to produce a VC as in [12], nanosecond vacuum discharge with a hollow cathode provides (after voltage is applied) automatic extraction of electron beams from the cathode and their further acceleration and injection into the anode area on the axis to form a VC (figure 1) [1, 2]. By analogy with POPS expressions we may estimate the fusion power $P_{\text{fusion}} \sim \varphi^2\theta^2 f^2\langle\sigma\upsilon\rangle l/\pi e^2 r_{\text{VC}}^2$ at the volume of nuclear burning for a reactor with cylindrical geometry [2] (l is the length of the cylinder). Assuming $\varphi \approx 60$ kV and $r_{\text{VC}} \approx 0.2$ cm, as well as $f^2 \sim 1, \theta_{\max} \leqslant 10^3, l \approx 0.3$–$0.5$ cm, we get the yield underestimation to $\sim 10^5$ neutrons for a single collapse of D^+ ions at the discharge axis or for one period of ions oscillations. Thus, a specific advantage of IECF systems such as POPS [12] or MFI [2] is the favorable scaling of fusion power (with a decreasing set-up size) which is increased with decreasing of r_{VC} and increasing of PW depth. As discussed above, during the total time of the voltage pulse applied we may get from single to 4–5 moments of deuterium ions collapses at the axis (depending on the relation between T_v and T_{pulse}). It will be accompanied by the corresponding number of neutron peaks in real experiments (see figures 5, 6 above and [2]) with the related structure and higher values of total neutron yield observed.

We remark that the frequency of neutron yield oscillations in vacuum discharge [2] is about ≈77–83 MHz, while extrapolation of POPS expressions [12] to A–C geometry and PW depth gives $\nu_{\text{POPS}} \approx 78$ MHz. It seems that this agreement is not accidental and confirms the similarity to POPS physics during some MFI regimes of nanoseconds vacuum discharge (where oscillations are exciting easily (figure 4 in [2] and figure 6 above) and are going without any special external drive). The miniature size ($r_{\text{VC}} \approx 0.2$ cm) as well as rather deep PW (like $\varphi \approx 50$–60 keV) corresponds to the extremely high fusion power densities $\left(\sim\varphi^2/r_{\text{VC}}^4\right)$ demonstrated at the present moment for the chosen system [2, 13] of table-top IECF. In the general case, besides beam–beam reactions (neutron yield estimated above), the other channels of IEC syntheses [15] like beam–background (neutrals), fast neutrals–background, beam–deuterium clusters, beam–anode (with deuterium) also have to be taken into account to estimate total neutron yield. In summary, fusion power of $\sim 10^{13}$ n/sec or higher would

be achievable. However, small absolute 'reactor' volume, the nanosecond scale of T_{pulse}, and losses restrict the total neutron yield, but keep it acceptable for some modern applications (perhaps, including small-scale hybrid reactors also).

Note that further PIC calculations of real neutron yields (besides other channels of DD reactions) have to take into account periodic compressions of the ionic subsystem as well as a more detail description of PW neutralization. This might provide at the collapse moments ion densities essentially higher than presented in figure 4 above (for similar POPS conditions the calculated value $n_{i\,\max} \sim 10^{19}$ cm^{-3}, and $r_{\min}$ at the compression moment is $\sim$60 μ [11]; our cylindrical geometry gives lower values of $n_{i\,\max}$ and the same order of $r_{\min}$). In addition to particle–particle syntheses, we remind the reader that VC is sometimes located inside a 'cloud' of burning 'dust' of different sizes and densities nucleated from anode material vapors (this has still not been included in PIC modeling). The total trapping of fast ions observed in experiment [2] would increase the neutron yield up to the order of magnitude (deuterium clusters target inside of PW with fast ions). A related example of a self-organized cluster ensemble is shown in figure 7. This shot and ensemble registered by CCD is similar to the presented one in figure 6 in [2] and manifests a high level pulsating neutron yield also ($\sim 5 \times 10^6/4\pi$ per 50 nanoseconds). Fast ions and even few keV hard x-rays are trapped there, and just neutrons are leaving these sorts of interelectrode ensembles (complex plasma microreactors). Negative and positive aspects of electrode erosion, as well as the fact that the PW is sometimes distorted by clusters fulfilled it, have to be analyzed in more detailed separately. Since for IEC systems $P_{\text{fusion}} \sim I^2$ and $Q_{\text{fusion}} \sim I$ [11], scaling by current ($\sim$1 kA) and changing the values of Q for different regimes of discharge need special discussion also. On the whole, the trapping of fast ions by interelectrode ensembles of clusters (including deuterium ones as potential targets), especially noticeable under effects of ensemble self-organizations (dusty stopping) represents additional opportunities as well as complexity for 'reactor' optimization.

Acknowledgments

We would like to thank G A Mesyats, A A Rukhadze, V E Fortov, N Ratakhin, A Evdokimov, G Maynard, N Granowski and Y Vitel for interest and support of the work as well as for stimulating discussions.

References

[1] Kurilenkov Y K *et al* 2000 *J. Physique* IV **10** Pr5–409
Kurilenkov Y K and Skowronek M 2003 *J. Phys. (Pramana, Indian Acad. Sci.)* **61** 1188
[2] Kurilenkov Y K, Skowronek M and Dufty J 2006 *J. Phys. A: Math. Gen.* **39** 4375
Kurilenkov Y K 2007 *Int. Workshop on Warm Dense Matter (WDM07) (France)* http://luli.polytechnique.fr/wdm07/program.html
[3] Ditmire T *et al* 1999 *Nature* **398** 489
Ditmire T 2000 *Phys. Rev. Lett* **84** 634
[4] Tarakanov V P 1992 *User's manuel for code KARAT* (Springfield, VA: Berkley Research Associates, Inc.)
Ignatov A M and Tarakanov V P 1994 *Phys. Plasmas* **1** 741
[5] Dubinov A E, Kornilova I Yu and Selemir V D 2002 *Usp. Phys. Nauk* **172** 1225
[6] Barengol'ts S A, Mesyats G A and Perel'shtein E A 2000 *JETPh* **91** 1176
[7] Plyutto A A 1960 *JETPh* **12** 1106
Plyutto A A 1970 *J. Technol. Phys.* **40** 2534
[8] Lavrent'ev O 1963 *Ukr. Phys. J.* **8** 440
Bondarenko B D 2001 *Usp. Phys. Nauk* **171** 886
[9] Elmore W C *et al* 1959 *Phys. Fluids* **2** 239
Hirsch R L 1967 *J. Appl. Phys.* **38** 4522

[10] Onishi M *et al* 1997 *Nucl. Fusion* **37** 611
[11] Nebel R A and Barnes D C 1998 *Fusion Technol.* **38** 28
Nebel R A and Barnes D C 1998 *Phys. Plasmas* **5** 2498
[12] Nebel R A *et al* 2005 *Phys. Plasmas* **12** 012701
Park J *et al* 2005 *Phys. Plasmas* **12** 056315
[13] Kurilenkov Y K *et al* 2008 *Proc. 15th Int. Symp. on High Current Electronics (SHCE), (Tomsk, Russia)* p 463
Kurilenkov Y K *et al* 2009 *Prikladnaya Fizika* (in Russian) at press
[14] Bobrov Y K, Bistrov V P and Rukhadze A A 2005 Short communications (Physics) *Lebedev. Phys. Inst.* **N7** 23
[15] Murali S K, Cipiti B B, Santarius J F and Kulchinskii G L 2006 *Phys. Plasmas.* **13** 053111